Characterization of Electronic Transition Energies and Trigonal Distortion of the $(FeO_6)^{9-}$ Coordination Complex in the $Al_2O_3:Fe^{3+}$ System: A Simple Method for Transition-Metal Ions in a Trigonal Ligand Field

Kuang Xiao-Yu*,†,‡ and Lu Cheng*,†

Institute of Atomic and Molecular Physics, Sichuan University, Chengdu 610065, China, and International Centre for Materials Physics, Academia Science, Shenyang 110016, China

Received: May 4, 2006; In Final Form: August 8, 2006

A theoretical method for studying the inter-relationships between electronic and molecular structure has been proposed on the basis of the complete energy matrices of electron−electron repulsion, the ligand field, and the spin−orbit coupling for the d^5 configuration ion in a trigonal ligand field. As an application, the local distortion structure and temperature dependence of zero-field splitting for Fe^{3+} ions in the $Al_2O_3:Fe^{3+}$ system have been investigated. Our results indicate that the local lattice structure of the $(FeO_6)^{9-}$ octahedron in the $Al_2O_3:Fe^{3+}$ system has an elongated distortion and the value of distortion is associated with the temperature. The elongated distortion may be attributed to the facts that the Fe^{3+} ion has an obviously larger ionic radius than the Al^{3+} ion and the Fe^{3+} ion will push the two oxygen triangles upward and downward, respectively, along the 3-fold axis. By diagonalizing the complete energy matrices, we found that the theoretical results of electronic transition energies and EPR spectra for Fe^{3+} ions in the $Al_2O_3:Fe^{3+}$ system are in good agreement with the experimental findings. Moreover, to understand the detailed physical and chemical properties of the Al_2O_3, the theoretical values of the zero-field splitting parameters and the corresponding distortion parameters in the range 50 K $\leq T \leq$ 250 K are reported first.

I. Introduction

The inter-relationships between electronic and molecular structure is central to understanding chemical and physical processes.[1−3] In general, the transition-metal complex molecules may display various spin ground states, such as high-spin, low-spin or intermediate-spin states, depending on the relative strength of the ligand-field energy and the mean spin-pairing energy. In some special cases, i.e., when the ligand-field splitting energy becomes comparable with the mean spin-pairing energy, the spin transition phenomena, such as high-spin ↔ low-spin transition, high-spin ↔ intermediate-spin transition, or intermediate-spin ↔ low-spin transition, can be observed.[4−11] So a careful theoretical study to establish the inter-relationships between electronic and molecular structure would be important. In the present work, a theoretical method for determining the inter-relation for a d^5 configuration ion in a trigonal ligand field is proposed by diagonalizing the complete energy matrices and considering the second-order and fourth-order EPR parameters D and $(a - F)$ simultaneously. By this method, the local distortion structure and temperature dependence of zero-field splitting for Fe^{3+} ions in the $Al_2O_3:Fe^{3+}$ system have been investigated.

Al_2O_3 is one of the most widely studied metal oxides.[12] It is a very interesting catalyst for many chemical reactions, such as the dehydration of alcohols and polymerization processes.[13] Al_2O_3 molecules doped with transition-metal ions (Fe^{3+}, Mn^{2+}, Cr^{3+}, Ti^{3+}, etc.) are extremely important industrial materials with a wide range of applications, especially in high-pressure science.[14−25] In these materials, the transition-metal impurities have been known to introduce deep levels. These levels can strongly affect the optical and electrical properties, because the properties of the impurity ion, such as charge, mass, and size, are different from those of the replaced host ion and the local properties in the vicinity of impurity ion, such as local compressibility and local thermal expansion coefficients, are unlike those in the host crystal. For the technical application, it is necessary to understand the microstructure and the properties of the paramagnetic ions in these materials.

Electron paramagnetic resonance (EPR) is regarded as an effective tool to study the microstructure and the local environment around a substitution magnetic ion site in crystals.[26] The reason is the EPR spectra usually furnish highly detailed microscopic information about the structure of the defects. The EPR spectra of Fe^{3+} ions in the $Al_2O_3:Fe^{3+}$ system have been experimentally observed by many researchers, but there has so far been no systematical theory for their analysis.[14−20] The reason the previous theoretical results are not in quite good agreement with the observed values may be due to the oversimplification of the theoretical method. For instance, Zheng has studied the local structure of Fe^{3+} ions in the $Al_2O_3:Fe^{3+}$ system on the basis of the second-order zero-field splitting parameter D only.[27] His conclusion is that the Fe^{3+} ion does not occupy the Al^{3+} ion site exactly but is displaced from it along the 3-fold axis toward the empty octahedral site. However, he did not investigate the fourth-order zero-field splitting parameter $(a - F)$ of Fe^{3+} ions in the $Al_2O_3:Fe^{3+}$ system. It is well-known that for a d^5 configuration ion in a trigonal ligand field, the high-spin ground state is the $^6A_1$ state. To describe the $^6A_1$ ground-state splitting of the Fe^{3+} ions in the Al_2O_3:

* Correspondence author. Mailing address: Institute of Atomic and Molecular Physics, Sichuan University, Chengdu 610065, China. E-mail address: palc@163.com.

† Sichuan University.

‡ Academia Sinica.

10.1021/jp062724o CCC: $33.50
Published on Web 09/14/2006

Fe^{3+} system, the spin Hamiltonian should include three different zero-field splitting parameters a, D, and $(a - F)$. The parameter a relates to a fourth-order spin operator and represents a cubic component of the crystalline electric field. The parameters D and $(a - F)$ are, respectively, associated with the second-order and fourth-order spin operators and represent an axial component of the crystalline electric field that is axially symmetric about the C_3 axis. To explain more reasonably the distortion structure, herein, we suggest that the two zero-field splitting parameters D and $(a - F)$ should be simultaneously considered in the determination of the local distortion structure of Fe^{3+} ions in the Al_2O_3:Fe^{3+} system.

II. Theoretical Method

The EPR spectra of the d^5 configuration Fe^{3+} ion in a trigonal ligand field may be analyzed by employing the spin Hamiltonian[19,20]

$$\hat{H} = \beta\vec{S}\cdot g\cdot\vec{B}_0 + \frac{1}{3}b_2^0O_2^0 + \frac{1}{60}(b_4^0O_4^0 + b_4^3O_4^3) \qquad (1)$$

where the first term corresponds to the Zeeman interaction, the following terms represent the zero-field splitting effect, b_k^q are the EPR zero-field splitting parameters, O_k^q are the standard Stevens spin operators.[28] From the spin Hamiltonian the explicit expression of the energy levels in the ground state $^6A_1$ for a zero magnetic field is given as follows

$$E\left(\pm\frac{1}{2}\right) = \frac{1}{3}b_2^0 + \frac{3}{2}b_4^0 \mp \frac{1}{6}\left[(18b_2^0 - 3b_4^0)^2 + \frac{9}{10}(b_4^3)^2\right]^{1/2}$$

$$E\left(\pm\frac{3}{2}\right) = -\frac{2}{3}b_2^0 - 3b_4^0$$

$$E\left(\pm\frac{5}{2}\right) = \frac{1}{3}b_2^0 + \frac{3}{2}b_4^0 \pm \frac{1}{6}\left[(18b_2^0 - 3b_4^0)^2 + \frac{9}{10}(b_4^3)^2\right]^{1/2} \qquad (2)$$

Then, the zero-field splitting energies ΔE_1 and ΔE_2, which are energies between the three Kramers doublets of the $S = {}^5/_2$ spin state, may be expressed as a function of the EPR parameters b_2^0, b_4^0 and b_4^3 [29]

$$\Delta E_1 = E\left(\pm\frac{5}{2}\right) - E\left(\pm\frac{1}{2}\right) = \pm\frac{1}{3}\left[(18b_2^0 - 3b_4^0)^2 + \frac{9}{10}(b_4^3)^2\right]^{1/2}$$

$$\Delta E_2 = E\left(\pm\frac{3}{2}\right) - E\left(\pm\frac{1}{2}\right) = -b_2^0 - \frac{9}{2}b_4^0 \pm \frac{1}{6}\left[(18b_2^0 - 3b_4^0)^2 + \frac{9}{10}(b_4^3)^2\right]^{1/2} \qquad (3)$$

where the positive and negative signs in eq 3 correspond to $b_2^0 \geq 0$ and $b_2^0 < 0$, respectively. It is noteworthy to mention that the parameters b_k^q are related to the EPR parameters a, D, and $(a - F)$. a is the cubic field splitting parameter, and D and $(a - F)$ correspond to axial component of the second-order and the fourth-order, respectively. The relationships are given by[30]

$$b_2^0 = D = 3B_2^0 \qquad b_4^0 = -\frac{a - F}{3} = 60B_4^0$$

$$b_4^3 = -\frac{20\sqrt{2}}{3}a = 60B_4^3 \qquad (4)$$

The perturbation Hamiltonian for a d^5 configuration ion in a trigonal symmetry may be expressed as[31]

$$\hat{H} = \hat{H}_{ee} + \hat{H}_{so} + \hat{H}_{cf} = \sum_{i<j} e^2/r_{i,j} + \zeta\sum_i l_i\cdot s_i + \sum_i V_i \qquad (5)$$

where the first term is the electron−electron interaction (represented, e.g., by the Racah parameters B and C), the second term is the spin−orbit coupling interaction (represented by the spin−orbit coupling coefficient ζ), and the third term is the ligand-field potential (represented, e.g., by the ligand-field parameters B_{kq}). The ligand-field potential V_i can be written as

$$V_i = \gamma_{00}Z_{00} + \gamma_{20}r_i^2Z_{20}(\theta_i,\phi_i) + \gamma_{40}r_i^4Z_{40}(\theta_i,\phi_i) + \gamma_{43}^c r_i^4 Z_{43}^c(\theta_i,\phi_i) + \gamma_{43}^s r_i^4 Z_{43}^s(\theta_i,\phi_i) \qquad (6)$$

where r_i, θ_i, and ϕ_i are spherical coordinates of the ith electron. Z_{lm}, Z_{lm}^c and Z_{lm}^s are defined as

$$Z_{l0} = Y_{l0}$$

$$Z_{lm}^c = (1/\sqrt{2})[Y_{l,-m} + (-1)^m Y_{l,m}]$$

$$Z_{lm}^s = (i/\sqrt{2})[Y_{l,-m} - (-1)^m Y_{l,m}] \qquad (7)$$

The $Y_{l,m}$ in eq 7 are the spherical harmonics. γ_{l0}, γ_{lm}^c, and γ_{lm}^s are associated with the local lattice structure around d^5 configuration ion by the relations

$$\gamma_{l0} = -\frac{4\pi}{2l+1}\sum_{\tau=1}^{n}\frac{eq_\tau}{R_\tau^{l+1}}Z_{l0}(\theta_\tau,\varphi_\tau)$$

$$\gamma_{lm}^c = -\frac{4\pi}{2l+1}\sum_{\tau=1}^{n}\frac{eq_\tau}{R_\tau^{l+1}}Z_{lm}^c(\theta_\tau,\varphi_\tau)$$

$$\gamma_{lm}^s = -\frac{4\pi}{2l+1}\sum_{\tau=1}^{n}\frac{eq_\tau}{R_\tau^{l+1}}Z_{lm}^s(\theta_\tau,\varphi_\tau) \qquad (8)$$

where θ_τ and φ_τ are angular coordinates of the ligand. τ and q_τ represent the τth ligand ion and its effective charge, respectively. R_τ denotes the impurity-ligand distance.

According to the irreducible representations $\Gamma_4(\Gamma_5)$ and Γ_6 of the C_3^* double group, three 84×84 energy matrices for a d^5 configuration ion corresponding to the perturbation Hamiltonian (5) have been constructed.[31] The matrix elements are the function of the Racah parameters B and C, Trees correction α, Racah correction β, the spin−orbit coupling coefficient ζ, and the ligand-field parameters B_{20}, B_{40}, B_{43}^c, and B_{43}^s, which are in the following forms[32]

$$B_{20} = \frac{1}{2}\sum_\tau G_2(\tau)(3\cos^2\theta_\tau - 1)$$

$$B_{40} = \frac{1}{8}\sum_\tau G_4(\tau)(35\cos^4\theta_\tau - 30\cos^2\theta_\tau + 3)$$

$$B_{43}^c = \frac{\sqrt{35}}{4}\sum_\tau G_4(\tau)(\sin^3\theta_\tau\cos\theta_\tau\cos 3\phi_\tau)$$

$$B_{43}^s = i\frac{\sqrt{35}}{4}\sum_\tau G_4(\tau)(\sin^3\theta_\tau\cos\theta_\tau\sin 3\phi_\tau) \qquad (9)$$

For Fe^{3+} ions in the Al_2O_3:Fe^{3+} system, the local structure is composed of two asymmetry three-edge pyramids and the Fe^{3+}

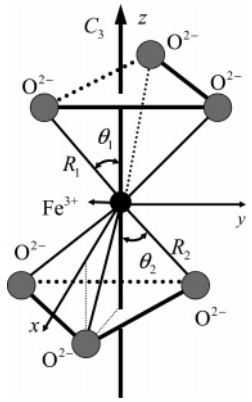

Figure 1. Local structure of the $(FeO_6)^{9-}$ coordination complex in the Al_2O_3:Fe^{3+} system. R_1 and R_2 are Fe−O bond lengths, θ_1 and θ_2 are the angles between the Fe−O bond and the C_3 axis when the Fe^{3+} ion replaces the Al^{3+} ion.

TABLE 1: Observed and Calculated Electronic Transition Energies of α-Fe_2O_3 (All Values in cm^{-1})

state	obsd[a]	calc[b]
$^4T_1(^4G)$	11600	11602.7
$^4T_2(^4G)$		17029.9
$^4E,^4A_1(^4G)$	23800	23803.3
$^4T_2(^4D)$		25039.1
$^4E(^4D)$	26700	26274.9
$^4T_1(^4P)$	31800	31461.3
$^4A_2(^4F)$		34248.2

[a] Reference 36. [b] $N = 0.9266$, $B = 815.31$ cm^{-1}, $C = 2891.19$ cm^{-1}, $\alpha = 59.71$ cm^{-1}, $\beta = -21.38$ cm^{-1}, $Dq = 1487.13$ cm^{-1}.

ion is surrounded by six oxygen ions. To describe the distortion, the Z axis is chosen along 3-fold axis, as shown in Figure 1. According to the superposition model,[33] the ligand-field parameter B_{43}^s will vanish and the $G_2(\tau)$ and $G_4(\tau)$ can be derived as

$$G_2(\tau) = eq_\tau G^2(\tau)$$

$$G_4(\tau) = eq_\tau G^4(\tau)$$

$$G^k(\tau) = \int_0^R R_{3d}{}^2(r) r^2 \frac{r^k}{R^{k+1}}\,dr + \int_R^\infty R_{3d}{}^2(r) r^2 \frac{R^k}{r^{k+1}}\,dr \quad (10)$$

The R in eq 10 and θ in eq 9 denote the Fe−O distance and the angle between Fe−O bond and C_3 axis, respectively. According to the Van Vleck approximation for $G^k(\tau)$ integral,[34] we may obtain the following relations

$$G_2(\tau) = \frac{-eq_\tau\langle r^2\rangle}{R^3} = \frac{A_2}{R^3} \qquad G_4(\tau) = \frac{-eq_\tau\langle r^4\rangle}{R^5} = \frac{A_4}{R^5} \quad (11)$$

where $A_2 = -eq_\tau\langle r^2\rangle$, $A_4 = -eq_\tau\langle r^4\rangle$, and $A_2/A_4 = \langle r^2\rangle/\langle r^4\rangle$. The ratio $\langle r^2\rangle/\langle r^4\rangle = 0.097$ is obtained from the radial wave function of the Fe^{3+} ion in complexes.[35] A_4 as a constant for the $(FeO_6)^{9-}$ octahedron can be determined from the electronic transition energies and the Fe−O band length of the α-Fe_2O_3 crystal.[36,37] By fitting the calculated electronic transition energies to the observed values, we obtain $A_4 = 27.6967$ au, $A_2 = 2.6870$ au, and $N = 0.9266$ for the $(FeO_6)^{9-}$ octahedron. The quantitative calculation results compared with the observed values are given in Table 1. Thus, when these values are substituted into eqs 9−11, the local distortion structure of Fe^{3+} ions in the Al_2O_3:Fe^{3+} system can be determined from the electronic transition

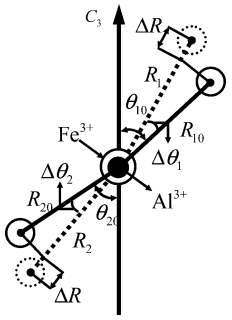

Figure 2. Local structure distortion for Fe^{3+} ions in the Al_2O_3:Fe^{3+} system. R_{10} and R_{20} are the Al−O bond lengths of Al_2O_3. θ_{10} and θ_{20} are the angles between the Al−O bond and the C_3 axis. $\Delta\theta_1$, $\Delta\theta_2$, and ΔR represent the structure distortion.

TABLE 2: Observed and Calculated Electronic Transition Energies of Fe^{3+} Ions in the Al_2O_3:Fe^{3+} System (All Values in cm^{-1})

state	obsd[a]	calc[b]
$^4T_1(^4G)$	9450	9453.2
$^4T_2(^4G)$	14350	14340.2
$^4E,^4A_1(^4G)$	22270	22269.6
$^4T_2(^4D)$	25510	25573.2
$^4E(^4D)$	26800	26811.1
$^4T_1(^4P)$	32500	32507.0
$^4A_2(^4F)$		34691.1

[a] Reference 36. [b] $N = 0.9113$, $B = 762.78$ cm^{-1}, $C = 2704.91$ cm^{-1}, $\alpha = 55.86$ cm^{-1}, $\beta = -20.00$ cm^{-1}, $Dq = 1545.46$ cm^{-1}.

energies and the spin Hamiltonian parameters can be obtained from the EPR spectra by diagonalizing the complete energy matrices.

III. Calculation for Fe^{3+} Ions in the Al_2O_3:Fe^{3+} Complex System

The local structure of Al_2O_3 is rhombohedral symmetry and it belongs to the space group D_{3d}^6 or equivalently $R\bar{3}c$.[38] In the Al_2O_3 lattice, the cations are located at the center of a slightly distorted octahedron of six oxygen ions. When the transition-metal Fe^{3+} ion is doped into the Al_2O_3, it will substite for the Al^{3+} ion in the octahedral site. The local lattice structure displays a trigonal distortion, which can be described bytwo parameters $\Delta\theta_1$ and $\Delta\theta_2$ (see Figure 2). We use the following relationship to evaluate the Fe−O bond lengths in the Al_2O_3:Fe^{3+} system.

$$R_1 = R_{10} + \Delta R \qquad R_2 = R_{20} + \Delta R \quad (12)$$

where $R_{10} = 1.966$ Å and $R_{20} = 1.857$ Å are the Al−O bond lengths of Al_2O_3. $\Delta R = 0.02918$ Å is determined by the electronic transition energies of Fe^{3+} ions in the Al_2O_3:Fe^{3+} system,[36] which is fixed in the following EPR calculation.

$$\theta_1 = \theta_{10} + \Delta\theta_1 \qquad \theta_2 = \theta_{20} + \Delta\theta_2 \quad (13)$$

θ_{10} and θ_{20} are the angles between the Al−O bond and the C_3 axis. Thus, the trigonal ligand-field parameters (B_{20}, B_{40}, B_{43}^c) are only the functions of $\Delta\theta_1$ and $\Delta\theta_2$. To decrease the number of adjustable parameters and to reflect the covalency effects, we use Curie et al.'s covalent theory[39] and take an average covalence factor N to determine the optical parameters as follows

$$B = N^4B_0 \qquad C = N^4C_0 \qquad \alpha = N^4\alpha_0 \qquad \beta = N^4\beta_0 \qquad \zeta = N^2\zeta_0 \quad (14)$$

The values of the free-ion parameters for the Fe^{3+} ion have

TABLE 3: Ground-State Zero-Field Splitting ΔE_1, ΔE_2 and the EPR Parameters b_2^0 and b_4^0 in the Temperature Range 4.2 K $\leq T \leq$ 300 K for Fe^{3+} Ions in the $Al_2O_3:Fe^{3+}$ System, where $10^4\Delta E_1$, $10^4\Delta E_2$, $10^4 b_2^0$, and $10^4 b_4^0$ Are in Units of cm^{-1}

T (K)	$\Delta\theta_1$ (deg)	$\Delta\theta_2$ (deg)	$10^4\Delta E_1$	$10^4\Delta E_2$	10^4	$b_2^0 10^4$	$b_4^0(10^4 b_2^0)_{exp}$	$(10^4 b_4^0)_{exp}$
4.2	−4.237	−1.471	10451.1	4015.2	1719.4	−113.1	1719[a]	−113[a]
							1719.2[b]	−113.8[b]
77	−4.341	−1.467	10435.6	4007.0	1716.6	−112.4	1716[a]	−112.3[a]
80	−4.301	−1.466	10445.5	4011.3	1718.2	−112.6	1718.2[b]	−112.6[b]
290	−4.552	−1.520	10245.5	3939.6	1684.1	−111.3	1684[a]	−111.3[a]
293	−5.035	−1.425	10360.7	3960.7	1705.0	−107.8	1705[c]	−108[c]
299	−4.826	−1.507	10209.0	3919.6	1679.0	−109.8	1679[a]	−109.7[a]
							1678.5[b]	−110.0[b]
300	−4.768	−1.504	10231.1	3927.7	1683.0	−110.0	1683[d]	−110[d]

[a] Reference 14. [b] Reference 15. [c] References 16 and 17. [d] References 18−20.

TABLE 4: Second-Order Zero-Field Splitting Parameter b_2^0 and Fourth-Order Zero-Field Splitting Parameter b_4^0 in the Range 50 K $\leq T \leq$ 250 K for Fe^{3+} Ions in the $Al_2O_3:Fe^{3+}$ System as a Function of the Two Parameters $\Delta\theta_1$ and $\Delta\theta_2$, where $10^4 b_2^0$ and $10^4 b_4^0$ Are in Units of cm^{-1}

T (K)	$\Delta\theta_1$ (deg)	$\Delta\theta_2$ (deg)	$10^4\Delta E_1$	$10^4\Delta E_2$	10^4	$b_2^0 10^4$	$b_4^0(10^4 b_2^0)_{exp}$ [a]	$(10^4 b_2^0)_{cacl}$ [b]
50	−4.291	−1.468	10433.5	4011.1	1717.8	−112.7		
100	−4.371	−1.467	10424.8	4002.0	1714.8	−112.1	1715	1714
150	−4.456	−1.477	10337.0	3984.7	1706.9	−111.8		
200	−4.505	−1.491	20329.9	3968.0	1699.1	−111.6	1698	1701
250	−4.615	−1.493	10296.7	3953.7	1693.7	−110.9		

[a] Reference 42. [b] Reference 43.

been obtained as $B_0 = 1106\ cm^{-1}$, $C_0 = 3299\ cm^{-1}$, $\alpha = 81\ cm^{-1}$, $\beta = -29\ cm^{-1}$, and $\zeta_0 = 470\ cm^{-1}$.[40] For Fe^{3+} ions in the $Al_2O_3:Fe^{3+}$ system, by diagonalizing the complete energy matrices, the electronic transition energies and ground-state zero-field splitting can be calculated with use of distortion parameters $\Delta\theta_1$ and $\Delta\theta_2$ and the covalence factor N. The comparisons between calculation and experiment of the electronic transition energies and EPR parameters for Fe^{3+} ions in the $Al_2O_3:Fe^{3+}$ system at different temperatures is listed in Tables 2 and 3. It can be seen from Table 3 that the theoretical results can agree well with the EPR experimental findings and the distortion angles $\Delta\theta_1 = -4.237°$ to $-5.035°$, $\Delta\theta_2 = -1.425°$ to $-1.520°$ are found for the temperature range 4.2−300 K. We also note that the local tilting angles θ_1 and θ_2 for Fe^{3+} ions in the $Al_2O_3:Fe^{3+}$ system are smaller than the corresponding host angles. This may be partly because the Fe^{3+} ion has an ionic radius ($r_{Fe^{3+}} = 0.645$ Å) obviously larger than Al^{3+} ($r_{Al^{3+}} = 0.535$Å)[41] and the Fe^{3+} ion will push the two oxygen triangles to move upward and downward, respectively, along the 3-fold axis and this will lead to a local elongated effect of the sublattice.

IV. Temperature Dependence of Zero-Field Splitting

The temperature dependence of the EPR spectra of Fe^{3+} ions in the $Al_2O_3:Fe^{3+}$ system has been measured by Geifman et al.[42] They found that the temperature has an important influence on the change of the zero-field splitting parameters. By comparing the temperature dependence of the relative change in the zero-field splitting parameters with that of the relative change in the linear dimensions of Al_2O_3, Geifman et al. assumed that the thermal expansion of a crystal makes the main contribution to the temperature dependence of zero-field splitting. On the basis of this assumption, Zheng et al. has made a theoretical investigation of D (or b_2^0) for d^5 ions in trigonal symmetry by using the high-order perturbation formulas.[43] The temperature dependence of the zero-field splitting parameter b_4^0 has not yet been investigated. Considering the information of the temperature dependent on zero-field splitting is useful in understanding the strength of coupling of the Fe^{3+} ion to the Al_2O_3 lattice and accordingly in understanding the changes of other properties induced by the Fe^{3+} impurity, it is important to make a theoretical analysis of the temperature dependence of the splitting parameters b_2^0 and b_4^0. From Table 3, we can see that parameters b_2^0 and b_4^0 are strongly dependent on the temperature, and the relations of zero-field splitting parameters dependent on the temperature are plotted in Figure 3. We can see that the parameter b_2^0 exhibits linear temperature dependence for 75 K $\leq T \leq$ 250 K, and the reasonable estimation for the values of the zero-field splitting parameters b_2^0 and b_4^0 in the temperature rang 50 K $\leq T \leq$ 250 K can be made from Figure 3. For the sake of simplicity, the results are given in Table 4. Substituting the covalence factor $N = 0.9113$ into the eq 14, we can get the optical parameters $B = 762.78\ cm^{-1}$, $C = 2704.91\ cm^{-1}$, $\alpha = 55.86\ cm^{-1}$, $\beta = -20.00\ cm^{-1}$, and $\zeta = 390.32\ cm^{-1}$. By use of eqs 2−3 and the optical parameters B, C, α, β, and ζ, we can calculate the corresponding local structure distortion parameters $\Delta\theta_1$ and $\Delta\theta_2$ in the temperature range 50

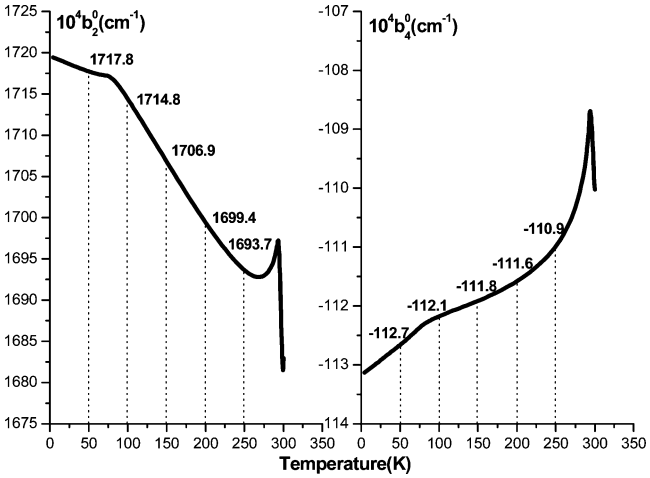

Figure 3. Temperature dependence of the second-order zero-field splitting parameter b_2^0 and fourth-order zero-field splitting parameter b_4^0 for Fe^{3+} ions in the $Al_2O_3:Fe^{3+}$ system.

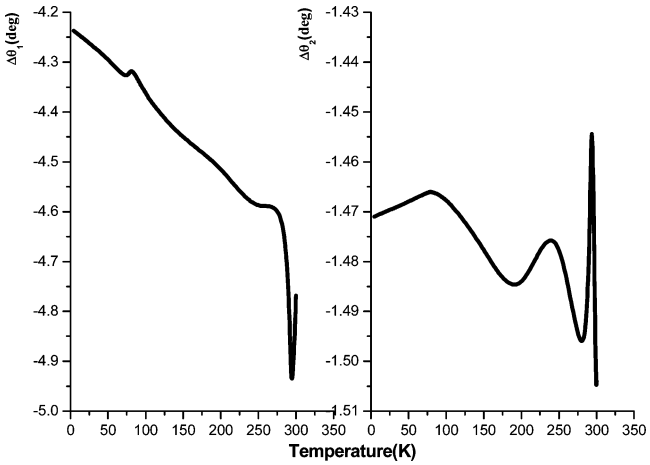

Figure 4. Temperature dependence of the local distortion structure parameters $\Delta\theta_1$ and $\Delta\theta_2$ for Fe^{3+} ions in the Al_2O_3:Fe^{3+} system.

$K \leq T \leq 250$ K by diagonalizing the complete energy matrices of the electron−electron repulsion, the ligand field, and the spin−orbit coupling of d^5 configuration ion in a trigonal ligand field. The results are also listed in Table 4. Although there may be some small errors in the calculated values of the local structure distortion parameters $\Delta\theta_1$ and $\Delta\theta_2$ because the parameters b_2^0 and b_4^0 are estimated from Figure 3, these values of $\Delta\theta_1$ and $\Delta\theta_2$ can be regarded as reasonable by comparison with those listed in Table 3. According to Tables 3 and 4, we can obtain the different distortion parameters $\Delta\theta_1$ and $\Delta\theta_2$ at different temperatures, and the relationships of $\Delta\theta_1$ and $\Delta\theta_2$ vs T are shown in Figure 4. It is found that the distortion parameters, $\Delta\theta_1$ and $\Delta\theta_2$, have an anomalistic value in the neighborhood of $T = 300$ K. It should be also noted that the change of distortion parameter $\Delta\theta_2$ is slower than that of $\Delta\theta_1$.

Using the complete diagonalization method, we establish the relationship between electronic and molecular structures and study the local molecular structure of the coordination complex. Up to now, theoretical calculations indicate that the simple ligand field model is a good approximation for typical ionic crystals, such as $KZnF_3$:Fe^{3+} [44] and Al_2O_3:Fe^{3+} systems, whereas its predictive power is limited for strong covalent crystals, for instance, SiC:Fe^{3+} and SiC:Mn^{2+} systems. To our knowledge, no satisfactory theoretical results have been reported until now. In the present paper, the local distortion structure and temperature dependence of zero-field splitting for Fe^{3+} ions in ionic crystal Al_2O_3 have been investigated by the ligand field model and the distortion angles $\Delta\theta_1$, $\Delta\theta_2$ versus temperature T are obtained. Of course, our theoretical results remain to be checked by other more direct experiments.

V. Conclusion

From the above studies, we have the following conclusions:

(i) The electronic transition energies and electron paramagnetic resonance spectra of Fe^{3+} ions in the Al_2O_3:Fe^{3+} system have been studied by diagonalizing the complete energy matrices for a d^5 configuration ion in a trigonal ligand field. It is worth noting that the above theoretical study of electronic transition energies and EPR spectra provides powerful guidelines for future experimental studies aimed at pinpointing how exactly Fe enters into the Al_2O_3 environment.

(ii) The temperature dependence of zero-field splitting parameters b_2^0 and b_4^0 has been derived, and the theoretical values are in good agreement with the experimental findings.

(iii) The local distortion structure parameters $\Delta\theta_1$ and $\Delta\theta_2$ in different temperatures are determined. The results show that the local tilting angles θ_1 and θ_2 for Fe^{3+} substituting the Al^{3+} ion site are smaller than the corresponding host angles. Moreover, the theoretical value of the zero-field splitting parameters and the corresponding distortion parameters in the temperature range $50 \text{ K} \leq T \leq 250$ K are reported first. These parameters are of significance in broadening our understanding of the physical and chemical properties of Al_2O_3. Of course, careful experimental investigations, especially ENDOR experiments, are required to clarify the local structure around the Fe^{3+} ions in the Al_2O_3:Fe^{3+} system in detail.

Acknowledgment. We express our gratitude to Dr. Zhu Ben-Chao for many helpful discussions. This work was supported by the National Natural Science Foundation of China (No. 10374068) and the Doctoral Education Fund of Education Ministry (No. 20050610011) of China.

References and Notes

(1) Glaser, T.; Bertini, I.; Moura, J. J. G.; Hedman, B.; Hodgson, K. O.; Solomon, E. I. *J. Am. Chem. Soc.* **2001**, *123*, 4859.
(2) Lehnert, N.; Ho, R. Y. N.; Que, L., Jr.; Solomon, E. I. *J. Am. Chem. Soc.* **2001**, *123*, 8271.
(3) Randall, D. W.; George, S. D.; Holland, P. L.; Hedman, B.; Hodgson, K. O.; Tolman, W. B.; Solomon, E. I. *J. Am. Chem. Soc.* **2000**, *122*, 11632.
(4) Kahn, O.; Martinez, C. J. *Science* **1998**, *279*, 44.
(5) Zhu, D.; Xu, Y.; Yu, Z.; Guo, Z.; Sang, H.; Liu, T.; You, X. *Chem. Mater.* **2002**, *14*, 838.
(6) Garcia, Y.; Ksenofontov, V.; Campbell, S. J.; Lord, J. S.; Boland, Y.; Gütlich, P. *J. Phys. Chem. B* **2004**, *108*, 17838.
(7) Roubeau, O.; Haasnoot, J. G.; Codjovi, E.; Varret, F.; Reedijk, J. *Chem. Mater.* **2002**, *14*, 2559.
(8) Jeftic, J.; Hauser, A. *J. Phys. Chem. B* **1997**, *101*, 10262.
(9) Boca, R.; Boca, M.; Dlhan, L.; Falk, K.; Fuess, H.; Haase, W.; Jarosciak, R.; Papankova, B.; Renz, F.; Vrbova, M.; Werner, R. *Inorg. Chem.* **2001**, *40*, 3025.
(10) Alberola, A.; Collis, R. J.; Humphrey, S. M.; Less, R. J.; Rawson, J. M. *Inorg. Chem.* **2006**, *45*, 1903.
(11) Zein, S.; Borshch, S. A. *J. Am. Chem. Soc.* **2005**, *127*, 16197.
(12) Ruberto, C.; Yourdshahyan, Y.; Lundqvist, B. I. *Phys. Rev. B* **2003**, *67*, 195412.
(13) Zdetsis, A. D.; Kunz, A. B. *Phys. Rev. B* **1982**, *26*, 4756.
(14) Bogle, G. S.; Symmons, H. F. *Proc. Phys. Soc.* **1959**, *73*, 531.
(15) Symmons, H. F.; Bogle, G. S. *Proc. Phys. Soc.* **1962**, *79*, 468.
(16) Buzaré, J. Y.; Silly, G.; Klein, J.; Scholz, G.; Stösser, R.; Nofz, M. *J. Phys.: Condens. Matter* **2002**, *14*, 10331.
(17) Nofz, M.; Stösser, R.; Scholz, G.; Dörfel, I.; Schultze, D. *J. Eur. Ceram. Soc.* **2005**, *25*, 1095.
(18) Morin, G.; Bonnin, D. *J. Magn. Reson* **1999**, *136*, 176.
(19) Priem, A.; Bentum, P. J. M.; Hagen, W. R.; Reijerse, E. J. *Appl. Magn. Reson.* **2001**, *21*, 535.
(20) Scholz, G.; Stösser, R.; Klein, J.; Silly, G.; Buzaré, J. Y.; Laligant, Y.; Ziemer, B. *J. Phys.: Condens. Matter* **2002**, *14*, 2101.
(21) Stösser, R.; Nofz, M.; Feist, M.; Scholz, G. *J. Solid State Chem.* **2006**, *179*, 652.
(22) Lee, S.; Brodbeck, C. M.; Yang, C. C. *Phys. Rev. B* **1977**, *15*, 2469.
(23) Krebs, J. J.; Maisch, W. G. *Phys. Rev. B* **1971**, *4*, 757.
(24) Matsunaga, K.; Nakamura, A.; Yamamoto, T.; Ikuhara, Y. *Phys. Rev. B* **2003**, *68*, 214102.
(25) Gaudry, E.; Kiratisin, A.; Sainctavit, P.; Brouder, C.; Mauri, F.; Ramos, A.; Rogalev, A.; Goulon, J. *Phys. Rev. B* **2003**, *67*, 094108.
(26) Keeble, D. J.; Loyo-Menoyo, M.; Furukawa, Y.; Kitamura, K. *Phys. Rev. B* **2005**, *71*, 224111.
(27) Zheng, W. C. *Physica B* **1998**, *245*, 119.
(28) Stevens, K. W. H. *Proc. Phys. Soc., London, Sect. A* **1952**, *65*, 209.
(29) Bleaney, B.; Abragam, A. *Electron Paramagnetic Resonance of Transition Ions*; Oxford University Press: Oxford, U.K., 1986.
(30) Nistor, S. V.; Goovaerts, E.; Schoemaker, D. *J. Phys.: Condens. Matter* **1994**, *6*, 2619.
(31) Kuang, X. Y. *Phys. Rev. B* **1987**, *36*, 797.
(32) Newman, D. J.; Urban, W. *Adv. Phys.* **1975**, *24*, 793.
(33) Newman, D. J.; Ng, B. *Rep. Prog. Phys.* **1989**, *52*, 699.
(34) Vleck, J. H. V. *Phys. Rev.* **1932**, *41*, 208.
(35) Kuang, X. Y.; Gou, Q. Q.; Zhou, K. W. *Phys. Lett. A* **2002**, *293*, 293.
(36) Sherman, D. M. *Phys. Chem. Miner.* **1985**, *12*, 161.

(37) Wyckoff, R. W. G. *Crastal Structures*; Interscience Publishers Ltd.: London, 1965; Vol. 2, Chapter V.
(38) Artman, J. O.; Murphy, J. C. *Phys. Rev.* **1964**, *135*, A1622.
(39) Curie, D.; Barthon, C.; Canny, B. *J. Chem. Phys.* **1974**, *61*, 3048.
(40) Kuang, X. Y.; Zhang, W.; Irène, M. B. *Phys. Rev. B* **1992**, *45*, 8104.
(41) Shannon, R. D. *Acta Crystallogr.* **1976**, A*32*, 751.
(42) Geifman, I. N.; Glinchuk, M. D. *Fiz. Tverd. Tela.* **1971**, *13*, 1050.
(43) Zheng, W. C.; Wu, S. Y. *J. Phys.: Condens. Matter* **1997**, *9*, 5081.
(44) Huang, X. F.; Kuang, X. Y.; Lu, W. *J. Phys. Chem. Solids.* **2005**, *66*, 109.